

CERN - European Organization for Nuclear Research

LCD-Note-2010-006

A Study of $e^+e^- \rightarrow H^0 A^0 \rightarrow b\bar{b}b\bar{b}$ at 3 TeV at CLIC

M. Battaglia^{*†}, P. Ferrari[‡]

^{*} CERN, Geneva, Switzerland,

[†] University of California at Santa Cruz, Santa Cruz, CA, USA

[‡] NIKHEF, Amsterdam, The Netherlands

June 22, 2010

Abstract

The precise determination of the masses of the CP-odd and -even heavy Higgs bosons is an important part of the study of Supersymmetry and its relation with cosmology through dark matter. This note presents a determination of the A^0 mass with the $e^+e^- \rightarrow H^0 A^0 \rightarrow b\bar{b}b\bar{b}$ process for a dark matter motivated cMSSM scenario with $M_A = 1141$ GeV at CLIC. The analysis is performed with full simulation and reconstruction at $\sqrt{s}=3$ TeV accounting for beamstrahlung effects. SM and SUSY backgrounds are considered and the effect of the overlay of $\gamma\gamma \rightarrow$ hadrons events on the signal is studied for various assumptions for the detector time-stamping capabilities. The di-jet mass resolution is improved by applying a kinematic fit. The A^0 mass can be determined with a statistical accuracy of $\simeq 3$ -5 GeV for 3 ab^{-1} of statistics and 0 to 20 bunch crossings of $\gamma\gamma$ background integrated in one event, respectively.

1 Introduction

The CLIC linear collider is expected to probe physics at the multi-TeV scale, complementing and extending the reach of the LHC on New Physics beyond the Standard Model. If this New Physics is manifested by a rich spectroscopic of new particles, as several models predict, their study will be a key part of the CLIC physics program. In this note we study the pair production of heavy supersymmetric Higgs bosons, $e^+e^- \rightarrow H^0 A^0 \rightarrow b\bar{b}b\bar{b}$ for the parameters of benchmark point K', defined in the constrained Minimal Supersymmetric Standard Model (cMSSM) extension in ref. [1]. This benchmark is characterised by very heavy supersymmetric particles, with kinematic thresholds for pair production between 2 and 3 TeV. The H^0 and A^0 bosons have masses of 1141 and 1137 TeV, respectively, with a natural width $\Gamma = 28$ GeV. The accurate determination of these masses is essential for outlining the SUSY profile and understanding the connection of SUSY with cosmology, through dark matter. The A^0 mass plays a special role in this respect. In fact, the relation between its mass, M_A , and that of the lightest neutralino, $M_{\chi_1^0}$, determines the cross section of the $\chi_1^0 \chi_1^0 \rightarrow A^0$ annihilation process in the early universe, which could have been responsible for determining the amount of relic dark matter we observe in the universe today [2]. Pair production of heavy neutral Higgs bosons at the linear collider has already been studied for several scenarios with lighter particles [3, 4]. This analysis is interesting for assessing the detector requirements in terms of b -tagging efficiency, since the signal has four b jets and small production cross section, jet clustering, di-jet invariant mass reconstruction and detector time stamping capabilities in presence of two-photon machine-induced background.

2 Event Simulation

For this study, signal events are generated with ISASUGRA 7.69 [5] and PYTHIA 6.125 [6]. The observed signal cross section at 3 TeV is 0.3 fb, accounting for the CLIC luminosity spectrum. The main SM background processes are generated with PYTHIA 6.125. In addition, the irreducible inclusive $b\bar{b}b\bar{b}$ SM background is generated with CompHep [7] at the parton level and subsequently hadronised with PYTHIA. The number of events generated for the various processes considered here and their cross sections are given in Table 1. Beamstrahlung effects are included using CALYPSO for the CLIC 2008 accelerator parameters [8]. We assume the beams to be unpolarised. Events are processed through full detector simulation using the GEANT-4-based MOKKA [9] program and reconstructed with MARLIN-based [10] processors assuming a version of the ILD detector [11], modified for physics at CLIC. A total of $\simeq 100k$ SM and SUSY events have been generated, fully simulated, reconstructed and analysed (see Table 1). Particle tracks are reconstructed by the combination of a Time Projection Chamber and a pixellated Si Vertex Tracker. The momentum resolution is $\delta p/p^2 = 2 \times 10^{-5} \text{ GeV}^{-1}$ and the impact parameter resolution $\sigma_{R-\Phi} = (5 \oplus \frac{15}{p_t(\text{GeV})}) \mu\text{m}$. The parton energy is reconstructed using the PANDORAPFA particle flow algorithm [12]. Performances are discussed below. For the $\gamma\gamma \rightarrow \text{hadrons}$ background simulation two photon events are generated with the GUINEA PIG program [13] using the 2008 nominal CLIC beam parameters at $\sqrt{s} = 3$ TeV where the hadronic background cross section is modelled following Schuler and Sjöstrand [14]. The energies of two colliding photons are stored with their relevant probability and passed to PYTHIA for the

Table 1: Summary of simulated samples

Process	σ (fb)	Generator	Nb of Events Generated
$H^0 A^0$	0.3	ISASUGRA 7.69+ PYTHIA 6.125	3000
Inclusive SUSY	32.5	ISASUGRA 7.69+ PYTHIA 6.125	20000
$H^+ H^-$	0.6	ISASUGRA 7.69+ PYTHIA 6.125	3000
$W^+ W^-$	464.9	PYTHIA 6.125	30000
$Z^0 Z^0$	26.9	PYTHIA 6.125	15000
$t\bar{t}$	19.9	PYTHIA 6.125	15000
$b\bar{b}b\bar{b}$	0.4	CompHEP+ PYTHIA 6.125	5000
$W^+ W^- Z^0$	32.8	PYTHIA 6.125	7500
$Z^0 Z^0 Z^0$	0.4	PYTHIA 6.125	2500

generation of the hadronic events. On average, there are 3.3 $\gamma\gamma \rightarrow \text{hadrons}$ events per bunch crossing (BX) with $M_{\gamma\gamma} > 3$ GeV. These are passed through the same MOKKA full detector simulation and overlayed to the particles originating from the primary e^+e^- interaction at the reconstruction stage, using the event overlay feature in the LCIO persistency package [15]. For this analysis, the $\gamma\gamma$ background is overlayed only to the signal $H^0 A^0$ events, in order to study its effect on the signal reconstruction and to the peaking $H^+ H^-$ background events. These samples are reconstructed with different amounts of overlayed background, corresponding to different time-stamping performances of the detector. The remaining backgrounds have a flat di-jet invariant mass distribution in the signal region and the discriminating variables adopted are not significantly affected by the two-photon background. The comparison of these results allows us to assess some requirements on the detector timing capabilities.

3 Event Selection and Reconstruction

At the chosen SUSY parameters, where the $e^+e^- \rightarrow H^0 A^0$ process is close to its kinematic threshold, the production cross section is small. The natural signal-to-background ratios to SM processes such as $W^+ W^-$ and $t\bar{t}$ are $\simeq 1/1500$ and $1/60$, respectively. Therefore, a set of selection criteria with rejection factors of $\mathcal{O}(10^3 - 10^4)$ must be applied. There are two main sets of cuts which effectively reduce the SUSY and SM backgrounds. The first is based on the event shape and jet multiplicity, since two-fermion and gauge boson pair production events at 3 TeV are highly boosted, while the heavy Higgs bosons of the signal are produced with small kinetic energy, giving 4-jet, spherical events. The second is b -tagging since all four jets in the signal sample contain b hadrons. The $b\bar{b}b\bar{b}$ irreducible SM background has a cross section of only

0.4 fb, which makes b -tagging the single most effective selection criterium to isolate the signal.

In order to reject particles which are poorly reconstructed or likely to originate from underlying $\gamma\gamma$ events, a set of minimal quality cuts are applied. Only particles with $p_t > 1$ GeV are considered, charged particles are also required to have at least 12 hits in the tracking detectors and $\delta p/p < 1$. The event selection proceeds as follows. First multi-jet hadronic events with little or no observed missing energy are selected. We require events to have at least 50 charged particles, total reconstructed energy exceeding 2.7 TeV, event thrust below 0.95, sphericity larger than 0.04, transverse energy exceeding 1.3 TeV and $3 < N_{\text{jets}} < 6$, where N_{jets} is the natural number of jets reconstructed using the Durham clustering algorithm [16] with $y_{\text{cut}} = 0.0025$. These cuts remove all the SUSY events with missing energy and the $e^+e^- \rightarrow f\bar{f}$ events.

For events fulfilling these criteria, we perform the final jet reconstruction using two different approaches and we study the sensitivity of the reconstruction techniques on the two-photon background. The first approach is to apply an exclusive reconstruction by forcing the event into four jets, as traditionally done in e^+e^- event reconstruction. Here, we use the Durham clustering algorithm and we shall refer to this as the “4-jet Durham” method. The second approach uses a more inclusive technique. Since $\gamma\gamma$ events give rise to soft jets, it appears advantageous to cluster jets using a method which behaves like a cone algorithm and select only the four most energetic jets for performing the di-jet reconstruction. We use the anti-kt clustering algorithm in cylindrical coordinates [17], implemented in the FastJet package, which we have ported as a processor in the Marlin analysis framework. The choice of cylindrical coordinates is optimal since the $\gamma\gamma \rightarrow \text{hadrons}$ events are forward boosted, similarly to the underlying events in pp collisions for which the anti-kt clustering has been optimised. For each event, we choose the minimum R value at which the event has exactly four jets with energy in excess of 150 GeV. These jets are then used for the reconstruction, while the lower energy jets, which are mostly due to the $\gamma\gamma$ events when the background is overlayed, are disregarded. We shall refer to this as the “semi-inclusive anti-kt” method. The effect of b -tagging selection is included for the reconstructed jets, requiring four jets to be b -tagged. For this analysis we use a parametrised response and we assume that the efficiency for jets containing decays products of b quarks, ε_b , is 0.85 with a mistag probability of 0.05 and 0.01 for c and light quarks, respectively. We study the dependence of the result on ε_b in Section 4. Then, the di-jet invariant mass is computed. Since there are three possible permutations for pairing the four selected jets and the H^0 and A^0 bosons are expected to be almost degenerate in mass, we take the combination minimising the difference ΔM of the two di-jet invariant masses and require $|\Delta M| < 190$ GeV. Since the signal events are predominantly produced in the central region while the $\gamma\gamma$ and some of the SM background events are forward peaked, we only accept events for which the jet with the minimum polar angle, θ , has $|\cos \theta| < 0.92$. Finally, events with one or more jets having an invariant mass within 12 GeV of the top mass are discarded, to reject $t\bar{t}$ and $H^+H^- \rightarrow t\bar{t}b\bar{b}$ backgrounds. The number of selected events for the signal and the main background processes at each stage of the event selection procedure is shown in Figure 1. We study the parton energy resolution for jets from signal events fulfilling our selection criteria. We compare the jet energy from particle flow to the energy of the b hadron which is closest in energy-momentum space. We study the distribution of the quantity $\frac{E_b - E_{\text{jet}}}{E_b}$ and we determine the r.m.s. of the distribution, truncated to include the 90% of the entries closest to the peak, RMS₉₀. We observe a relative parton

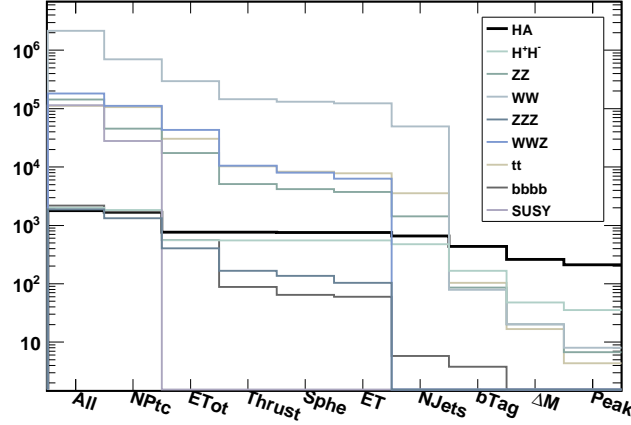


Figure 1: Number of selected di-jets for the signal and the main background processes at each stage of the event selection procedure

Table 2: RMS_{90} relative energy resolution for b -jets in signal events reconstructed with the 4-jet Durham clustering and the semi-inclusive anti-kt algorithm for different amounts of overlayed $\gamma\gamma$ background.

Nb of BX of overlayed $\gamma\gamma$	$\text{RMS}_{90}/E_{\text{jet}}$	
	4-jet Durham	semi-inclusive anti-kt
0	0.113 ± 0.002	0.112 ± 0.002
20	0.149 ± 0.003	0.129 ± 0.002
40	0.170 ± 0.003	0.133 ± 0.002
60	0.183 ± 0.003	0.140 ± 0.002

energy resolution $\text{RMS}_{90}/E_{\text{jet}} = 0.113 \pm 0.002$ and 0.112 ± 0.002 for jets from selected signal $H^0 A^0$ events in absence of overlayed background using the 4-jet Durham and the semi-inclusive anti-kt algorithms, respectively. This resolution is due to both the performance of the particle flow for jet energies as high as 1.3 TeV and also the effect of neutrinos produced in semileptonic heavy quark decays and escaping the detector.¹⁾ The evolution of the $\text{RMS}_{90}/E_{\text{jet}}$ resolution on the b -jets with the amount of overlayed $\gamma\gamma$ events for the two algorithms is summarised in Table 2.

The Higgs mass resolution is studied by fitting the di-jet invariant mass distribution with the

¹⁾Repeating the analysis for $H^0 A^0$ events where both bosons are forced to decay into light quark and into b quarks without semileptonic decays with escaping neutrinos we obtain a relative parton energy resolution $\text{RMS}_{90} = 0.088 \pm 0.002$ and $\text{RMS}_{90} = 0.093 \pm 0.004$, respectively.

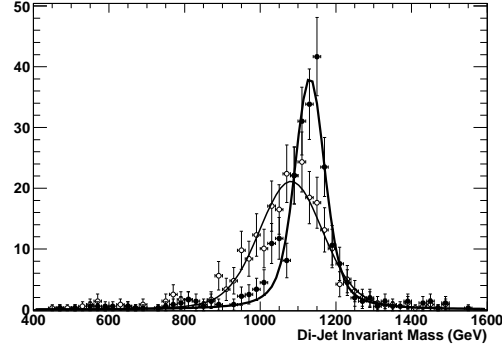


Figure 2: Di-jet invariant mass distribution for signal events before (open circles) and after (filled circles) kinematic fit using the semi-inclusive anti-kt jet clustering.

sum of two Breit-Wigner functions, describing the A^0 and H^0 signals, folded with a Gaussian resolution term. In this fit we set three parameters free: the A^0 mass, M_A , the Gaussian resolution term, σ_M , and the number of signal events, N_{signal} , while keeping the H^0 to A^0 mass splitting and the natural widths of the bosons fixed to their values in the SUSY model. We obtain a di-jet invariant mass resolution $\sigma_M = (68.5 \pm 6.2)$ GeV with the 4-jet clustering and (76.3 ± 6.3) GeV using the semi-inclusive anti-kt.

In order to improve the di-jet mass resolution, we apply a constrained kinematic fit. We use the port of the PUFITC kinematic fit algorithm [18] to the MARLIN framework. PUFITC was originally developed for W^+W^- reconstruction in DELPHI at LEP-2 and it has been successfully applied for the reconstruction of simulated linear collider events at lower energies [4]. The kinematic fit adjusts the momenta of the four jets as $p_F = ap_M + bp_B + cp_C$, where p_M is the jet momentum from particle flow, p_B and p_C are unit vectors transverse to p_M and to each other and a , b and c free parameters. The rescaled jet momenta minimise the quantity $\sum_i (\frac{(a_i - a_0)^2}{\sigma_a^2} + \frac{b_i^2}{\sigma_b^2} + \frac{c_i^2}{\sigma_c^2})$, where a^0 is the expected energy loss parameter, σ_a the energy spread and σ_b , σ_c the transverse energy spreads as in the notation used above. For this analysis, we impose the constraints $p_x = p_y = 0$ and $E \pm |p_z| = \sqrt{s}$, where the last conditions accounts for beamstrahlung photons radiated along the beam axis. We take the values of the energy spread from simulation. We only accept events with a kinematic fit $\chi^2 < 10$. After the kinematic fit, the relative jet energy resolution $\text{RMS}_{90}/E_{\text{jet}}$ improves to 0.094 ± 0.002 and to 0.103 ± 0.002 without and with 20 BX of $\gamma\gamma$ background, respectively. The di-jet invariant mass resolution improves by more than a factor of two to $\sigma_M = (27.7 \pm 4.8)$ GeV and (29.8 ± 4.7) GeV using the 4-jet and the semi-inclusive anti-kt method, respectively (see Figure 2). The use of a kinematic fit also mitigates the effect of the overlayed $\gamma\gamma$ events on the di-jet mass resolution. Since we do impose the nominal centre-of-mass energy, allowing for beamstrahlung, jet energies are rescaled in the fit. The Gaussian resolutions of the di-jet invariant masses obtained for the raw jet energy and momentum from the particle flow and that for the rescaled values after the kinematic fit are given in Table 3 for the two jet algorithms and different amounts of overlayed backgrounds. Up to about 20-30 BXs

Table 3: Higgs mass experimental width after kinematic fitting for different amounts of overlaid $\gamma\gamma$ background using the 4-jet Durham clustering and the semi-inclusive anti-kt algorithm.

Nb of BX of overlaid $\gamma\gamma$	Kinematic Fit $\sigma_{M_{jj}}$ (GeV)	
	4-jet	semi-incl.
0	27.7 ± 4.8	29.8 ± 4.7
5	32.0 ± 5.0	30.1 ± 5.0
20	54.0 ± 8.3	34.5 ± 6.7
40	72.2 ± 7.4	45.4 ± 5.6
60	78.6 ± 10.9	52.5 ± 8.2

the kinematic fit ensures a good di-jet invariant mass resolution. Above 40 BXs of background, corresponding to about 1.75 TeV of total energy from $\gamma\gamma \rightarrow \text{hadrons}$ events overlaid to the $e^+e^- \rightarrow H^0 A^0$ event, the di-jet mass resolution quickly degrades for the 4-jet cluster while it remains reasonably good for the semi-inclusive anti-kt algorithm.

4 Results

We consider the results of the analysis of a data set corresponding to an integrated luminosity of 3 ab^{-1} taken at $\sqrt{s} = 3 \text{ TeV}$, corresponding to the production of $\simeq 800 e^+e^- \rightarrow H^0 A^0$ events. The invariant mass distribution of the two di-jets in events selected by the criteria discussed above is shown in Figure 3 for various amounts of $\gamma\gamma$ background overlaid. The SM background is small and flat in the signal region. The only peaking background is represented by $H^+H^- \rightarrow t\bar{b}t\bar{b}$ events fulfilling the selection criteria. These poorly reconstructed charged Higgs decays passing the anti-top and jet selection criteria give di-jet masses centred at approximately the same mass as the H^0 and A^0 bosons, since $M^{H^\pm} = 1148 \text{ GeV}$ in this model, but with a broader distribution. We repeat the fit to the di-jet mass distribution adding a smooth background, parametrised by a second order polynomial and a peaking background term, parametrised by a Breit-Wigner distribution. We obtain the parameters of these distributions by fitting the distributions for the corresponding samples. The fitted number of signal, N_{signal} , and background, N_{bkg} , events and the M_A mass value after the kinematic fit for the various $\gamma\gamma$ overlay conditions are summarised in Table 4. We observe a significant advantage in using the semi-inclusive anti-kt method over the more traditional 4-jet clustering. While performances are comparable in absence of background, the statistical accuracy of the mass measurement is more stable with the amount of overlaid background when using the semi-inclusive anti-kt method. The A^0 mass is measured with a statistical accuracy of $\simeq 3 \text{ GeV}$ in absence of $\gamma\gamma$ background, which increases to $\simeq 5 \text{ GeV}$ for 20 BXs of overlaid background. A $\simeq 3 \sigma$ systematic upward shift of the fitted mass value for 20 or more bunch crossings of background, which appears for the 4-jet clustering method, is removed by using the semi-inclusive anti-kt clustering and the fitted mass remains

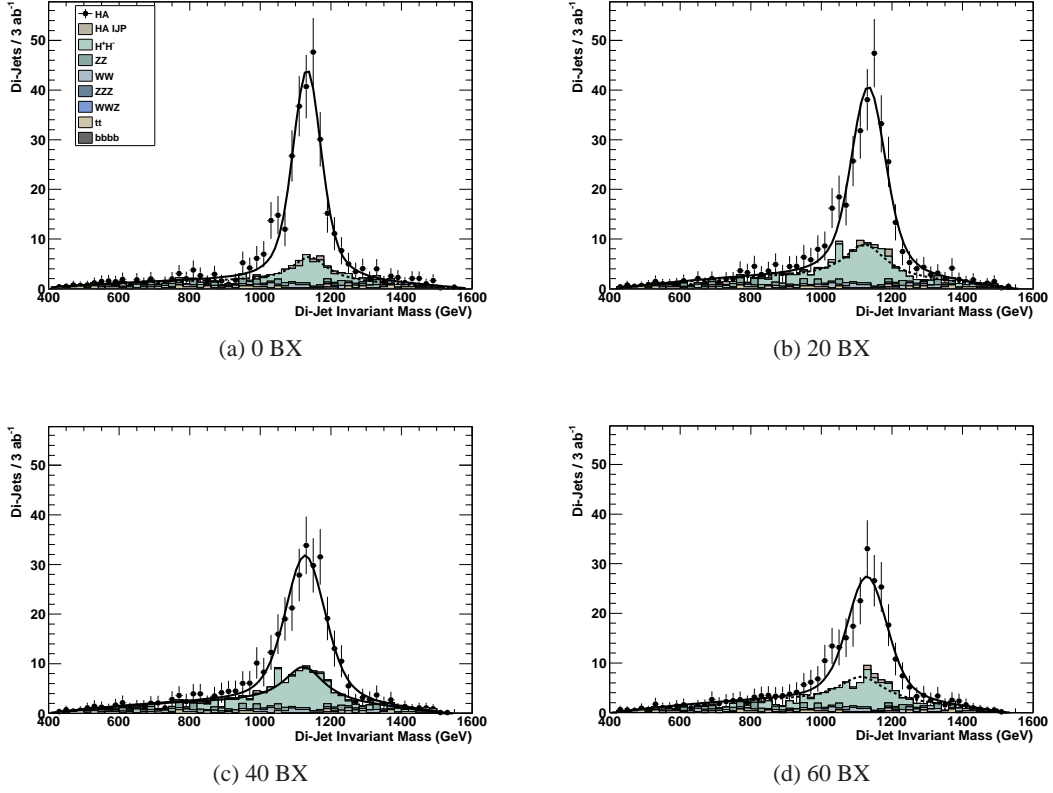


Figure 3: Di-jet invariant mass distribution for (a) no, (b) 20, (c) 40 and (d) 60 BXs of overlaid $\gamma\gamma$ background for 3 ab^{-1} of integrated luminosity at $\sqrt{s}=3 \text{ TeV}$. The HA signal, the HA events with incorrect jet pairing and the various background components are highlighted.

Table 4: Number of selected background and signal di-jets and value of the A^0 mass after kinematic fitting for different amounts of overlaid $\gamma\gamma$ background for 3 ab^{-1} of integrated luminosity at $\sqrt{s}=3 \text{ TeV}$.

Nb. of BXs of overlaid $\gamma\gamma$	N_{bkg}	N_{signal}	$M_A \text{ (GeV)}$	
			4-jet	semi-incl.
0	76	222 ± 19	1137.4 ± 3.3	1136.7 ± 3.4
5	77	224 ± 20	1144.4 ± 3.8	1135.9 ± 3.7
20	102	208 ± 20	1160.7 ± 6.9	1139.9 ± 5.4
40	96	183 ± 20	1167.2 ± 8.2	1134.1 ± 7.2
60	97	167 ± 21	1170.6 ± 9.7	1132.9 ± 8.6

within less than 1σ from its simulated value. Finally, we repeat the analysis by changing the b -

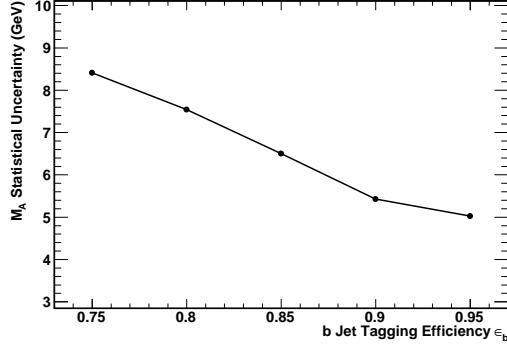


Figure 4: Statistical uncertainty on M_A as a function of the b -tagging efficiency per jet, ϵ_b , for 20 BX of $\gamma\gamma$ background overlaid.

tagging efficiency per jet, ϵ_b , in the range $0.75 < \epsilon_b < 0.95$ and study the change in the statistical accuracy on M_A as a function ϵ_b (see Figure 4).

5 Conclusions

The process $e^+e^- \rightarrow H^0 A^0 \rightarrow b\bar{b}b\bar{b}$ has been studied for the parameters of a dark matter motivated, high mass SUSY scenario with $M_A = 1141$ GeV. The analysis is based on fully simulated and reconstructed events and includes both physics backgrounds and machine-induced $\gamma\gamma$ events. CLIC at 3 TeV can study the production of pairs of heavy Higgs particles with high accuracy up to masses close to the production kinematic threshold. Event shape discriminating variables and jet flavour tagging efficiently reduce the SM and SUSY backgrounds to achieve a good signal-to-background ratio in the signal region at high mass. A semi-inclusive jet clustering using a cone-like algorithm in cylindrical coordinates helps in reducing the impact of overlaid events and ensure a stable, unbiased mass determination up to largest number of overlaid bunch crossings considered in this study. Due to the favourable kinematics of the signal events, the di-jet invariant mass resolution can be significantly improved by performing a constrained kinematic fit, accounting for beamstrahlung. This fit further mitigates the impact of overlaid $\gamma\gamma$ background up to $\simeq 20$ -30 BXs, corresponding to detector time stamping accuracies of 10-15 ns. Under these conditions, the A^0 mass can be determined with a statistical accuracy of ± 3 -5 GeV for an integrated luminosity of 3 ab^{-1} . This accuracy matches that required for obtaining predictions on the relic dark matter density in the universe from collider data with a precision comparable to that presently achieved in the study of the cosmic microwave background with the WMAP satellite data [19].

The results reported in this note can be further improved. The particle flow algorithm still needs to be optimised for jets of $\mathcal{O}(1 \text{ TeV})$. Explicit b -tagging has yet to be performed and can profit from the considerable decay length of the energetic b hadrons. The jet clustering algorithm

can be further optimised for the reconstruction of events in presence of a diffuse background, as in the case of a large number of overlayed $\gamma\gamma$ events.

6 Acknowledgements

We are grateful to the colleagues who contributed to this study. In particular, D. Schulte provided the luminosity spectrum and the $\gamma\gamma$ background events. E. Boos and S. Bunichev helped with the generation of events with CompHep. J. Quevillon studied jet clustering of HA events at the early stage of the analysis, while M. Cacciari guided us in the use of the anti-kt algorithm implemented in FastJet. D. Schlatter and A. Nomerotski carefully read the manuscript.

References

- [1] M. Battaglia, A. De Roeck, J. R. Ellis, F. Gianotti, K. A. Olive and L. Pape, Eur. Phys. J. C **33** (2004) 273 [arXiv:hep-ph/0306219].
- [2] J. R. Ellis, T. Falk, G. Ganis, K. A. Olive and M. Srednicki, Phys. Lett. B **510** (2001) 236 [arXiv:hep-ph/0102098].
- [3] E. Coniavitis, A. Ferrari, Phys. Rev. D **75** (2007) 015004.
- [4] M. Battaglia, B. Hooberman, N. Kelley, Phys. Rev. D **78** (2008) 015021.
- [5] F. E. Paige, S. D. Protopopescu, H. Baer and X. Tata, arXiv:hep-ph/0312045.
- [6] T. Sjostrand, S. Mrenna and P. Z. Skands, JHEP **0605** (2006) 026 [arXiv:hep-ph/0603175].
- [7] E. Boos *et al.* [CompHEP Collaboration], Nucl. Instr. and Meth. A **534** (2004), 250.
- [8] H. Braun *et al.* [CLIC Study Team], CLIC-NOTE-764 (2008).
- [9] P. Mora de Freitas, in Proc. of the *Int. Conf. on Linear Colliders (LCWS 04)*, Ed. de l'Ecole Polytechnique, Paris, 2004, vol. I, 437.
- [10] F. Gaede, Nucl. Instrum. Meth. A **559** (2006) 177.
- [11] H. Stoeck *et al.* [The ILD Concept Group], The International Large Detector - Letter of Intent, March 2009.
- [12] M. A. Thomson, Nucl. Instrum. Meth. A **611** (2009) 25 [arXiv:0907.3577 [physics.ins-det]].
- [13] D. Schulte, TESLA Note 97-08.
The $\gamma\gamma$ events have been generated by Daniel Schulte.
- [14] G. A. Schuler and T. Sjöstrand, CERN-TH/96-119.

- [15] F. Gaede, T. Behnke, R. Cassell, N. Graf, T. Johnson and H. Vogt, in Proc. of *Computing in high energy physics and nuclear physics*, Interlaken, 2004, 471.
- [16] S. Catani, Y. L. Dokshitzer, M. Olsson, G. Turnock and B. R. Webber, Phys. Lett. B **269** (1991) 432.
- [17] M. Cacciari, G. P. Salam and G. Soyez, JHEP **0804** (2008) 063 [arXiv:0802.1189 [hep-ph]].
- [18] P. Abreu *et al.* [DELPHI Collaboration] Eur. Phys. J. C **2** (1998) 581.
- [19] D. Larson *et al.*, arXiv:1001.4635 [astro-ph.CO].